5-23-2016

Effect of bed particle size on heat transfer between fluidized bed of group b particles and vertical rifled tubes

Artur Blaszczuk
Czestochowa University of Technology; Institute of Advanced Energy Technologies, Poland, ablaszczuk@is.pcz.czest.pl

Wojciech Nowak
AGH University Science and Technology, Poland

Jaroslaw Krzywanski
Jan Dlugosz University in Czestochowa, Poland

Czestochowa University of Technology,
Institute of Advanced Energy Technologies
ul. Dabrowskiego 73, 42-200 Czestochowa, POLAND

Effect of bed particle size on heat transfer between fluidized bed of group B particles and vertical rifled tubes

Artur Blaszczuk, **Wojciech Nowak*, Jaroslaw Krzywanski****

**AGH University of Science and Technology*

***Jan Dlugosz University in Czestochowa*

FLUIDIZATION XV
May 22-27th , 2016, Fairmont Le Chateau Montebello, Ontario, Canada

SCHEDULE A PRESENTATION

Introduction

- ✓ Key parameters for heat transfer conditions,
- ✓ Heat transfer mechanistic model.

Description of CFB facility (large scale)

- ✓ Arrangement of heating surfaces,
- ✓ Data of water membrane walls,
- ✓ Measuring ports of furnace data,
- ✓ Experimental conditions for all tests.

Results

- ✓ Temperature distribution vs furnace height,
- ✓ Solid suspension density profiles,
- ✓ Heat transfer coefficient distributions,
- ✓ Contribution of heat transfer mechanisms.

Conclusions

KEY PARAMETERS FOR HEAT TRANSFER CONDITIONS

Heat transfer behaviour inside furnace chamber can be depended on upon following parameters:

- **particle size distribution** of granular materials (i.e. fuel, sorbent, make-up sand),
- **suspension density**,
- **bed voidage**,
- **solid circulation rate**,
- **air staging**,
- **carbon dioxide concentration**,
- **circulation rate of bed material** between combustion chamber and return system,
- **fuel moisture content and heating value**.

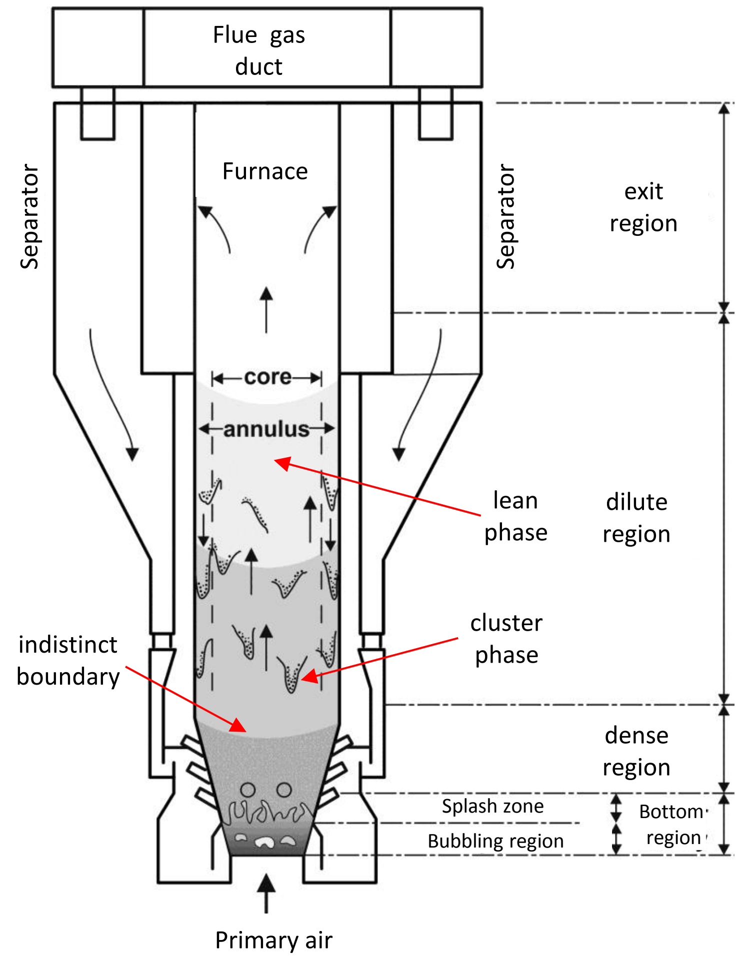

Fig. 1. Core annulus structure of CFB.

HEAT TRANSFER MECHANISTIC MODEL

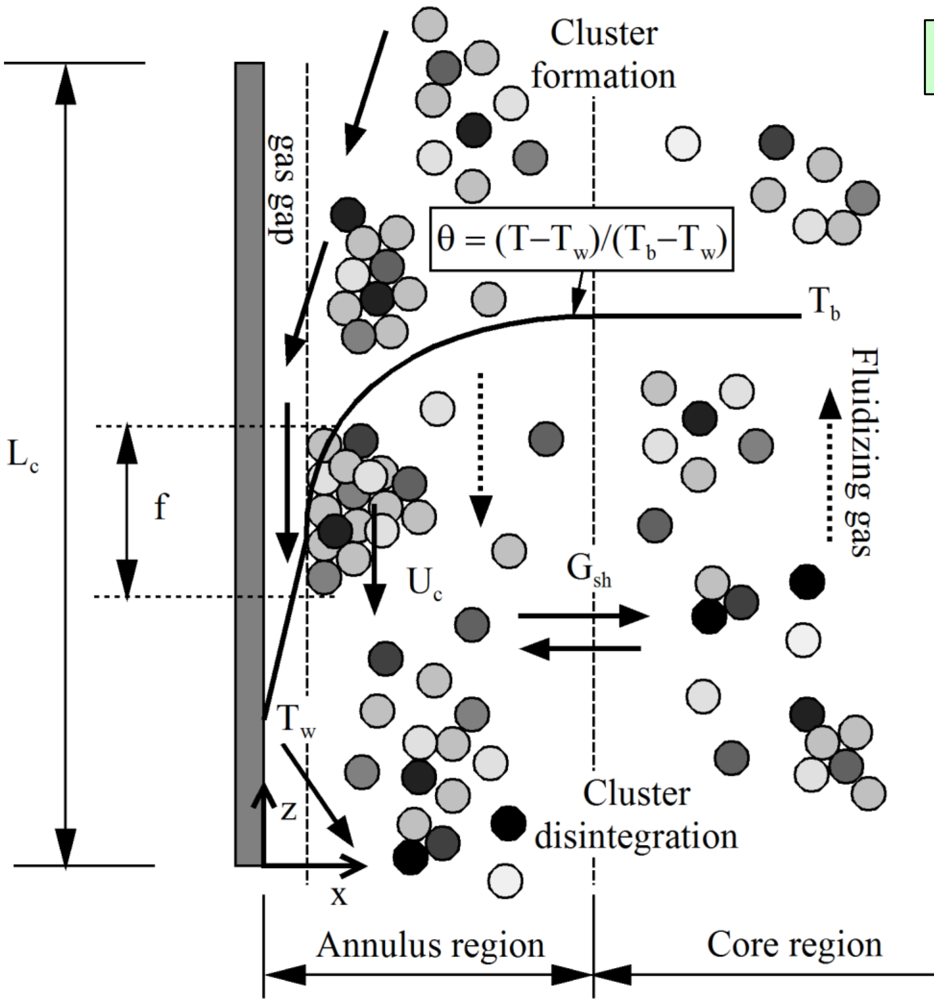

Fig. 2. Single cluster forms in the vicinity of the membrane wall inside CFB furnace [1, 2, 3].

$$h = h_{conv} + h_{rad} = f h_p + (1-f) h_g + f h_{rc} + (1-f) h_{rd}$$

$$f = 1 - \exp\left(-4300 \{1-\varepsilon\}^{1.39} \{D_h/H\}^{0.22}\right)$$

Convection components h_{conv}

$$h_p = \frac{1}{\left(\frac{\pi t_c}{4 k_c \rho_c c_c}\right)^{0.5} + \frac{d_p \delta}{k_g}}$$

$$h_g = \frac{k_g c_p}{d_p c_g} \cdot \left(\frac{\rho_d}{\rho_p}\right)^{0.3} \cdot \left(\frac{U_t^2}{g d_p}\right)^{0.21} \cdot \mathrm{Pr}$$

$$\rho_d = \rho_p Y + \rho_g (1-Y)$$

$$t_c = \frac{L_c}{U_c} = \frac{0.0178 \rho_b^{0.596}}{0.75 \cdot \left(\rho_p g d_p / \rho_g\right)^{0.5}}$$

$$\delta = 0.0282\, d_p (1-\varepsilon)^{-0.59}$$

$$\theta = \frac{T - T_w}{T_b - T_w} = 1 - \left[-0.023 \mathrm{Re}_p + 0.094 \left(\frac{T_b}{T_w}\right) + 0.294 \left(\frac{z}{H}\right)\right] \cdot \exp\left[-0.0054 \left(\frac{x}{d_p}\right)\right]$$

Radiation components h_{rad}

$$h_{rc} = \frac{\sigma \cdot \left(T_c^4 - T_w^4\right)}{\left(1/e_c + 1/e_w - 1\right) \cdot \left(T_c - T_w\right)}$$

$$h_{rd} = \frac{\sigma \cdot \left(T_b^4 - T_w^4\right)}{\left(1/e_d + 1/e_w - 1\right) \cdot \left(T_b - T_w\right)}$$

$$e_c = 0.5 (1 + e_p)$$

$$e_d = \left[\frac{e_p}{(1-e_p)0.5}\left(\frac{e_p}{(1-e_p)0.5} + 2\right)\right]^{0.5} - \frac{e_p}{(1-e_p)0.5}$$

[1] A. Blaszczuk, W. Nowak, Bed-to-wall heat transfer coefficient in a supercritical CFB boiler at different bed particle sizes, *Int. J. Heat Mass Transfer* 79 (2014) 736–749.
[2] A. Blaszczuk, W. Nowak, Heat transfer behavior inside a furnace chamber of large-scale supercritical CFB reactor, *Int. J. Heat Mass Transfer* 87 (2015) 464–480.
[3] A. Blaszczuk, W Nowak, Sz. Jagodzik, Bed-to-wall heat transfer in a supercritical circulating fluidised bed boiler, *Chem. Process Eng.* 35(2) (2014) 191-204.

ARRANGEMET OF HEATING SURFACES

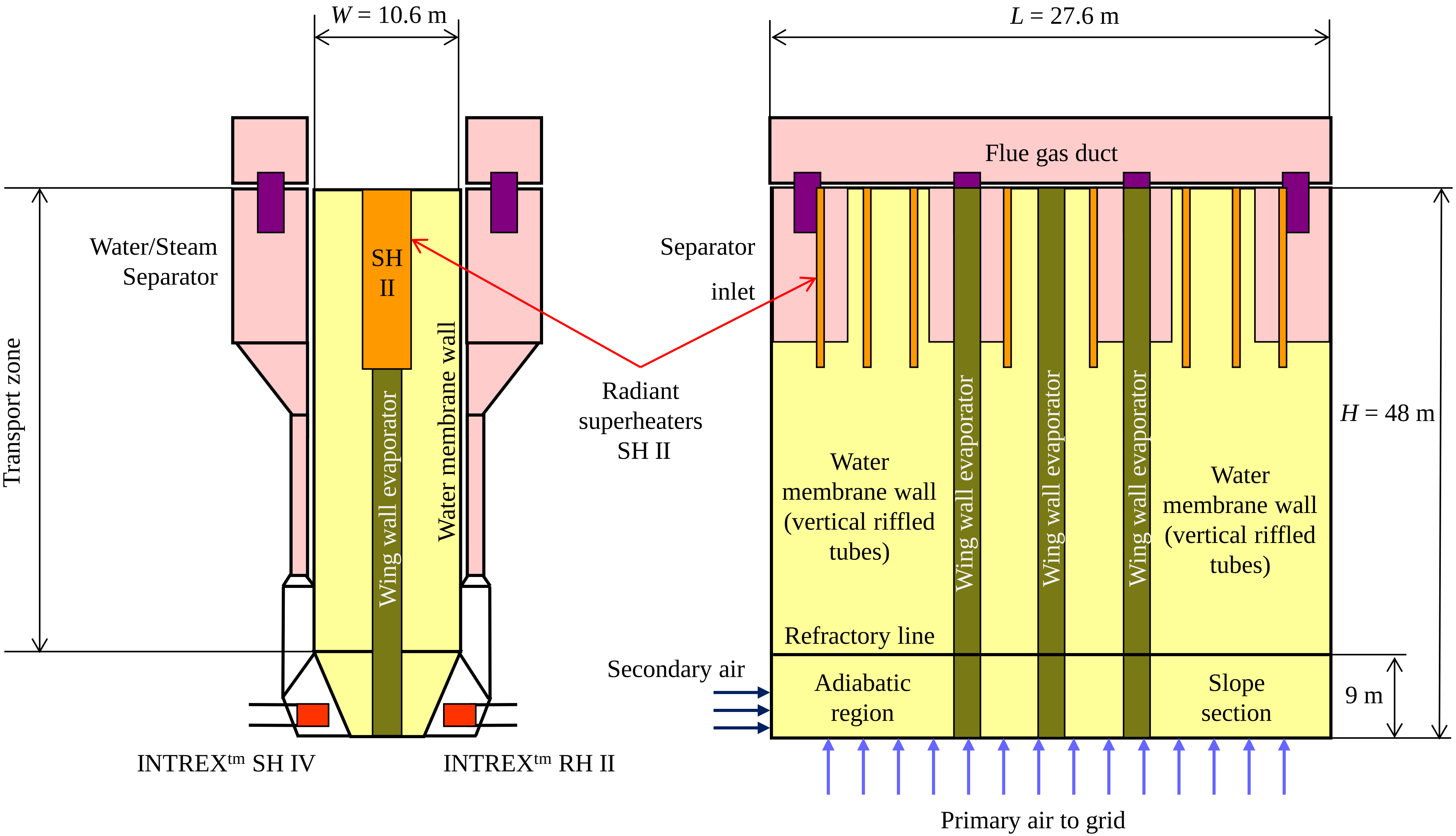

Fig. 3. Arrangement of heating surfaces in circulating fluidized bed boiler with steam capacity 1296t/h [4].

[4] A. Blaszczuk, J. Leszczynski, W. Nowak, Simulation model of the mass balance in a supercritical circulating fluidized bed combustor, *Powder Technol.* 246 (2013) 313–326.

DATA OF WATER MEMBRANE WALLS (vertical riffled tubes)

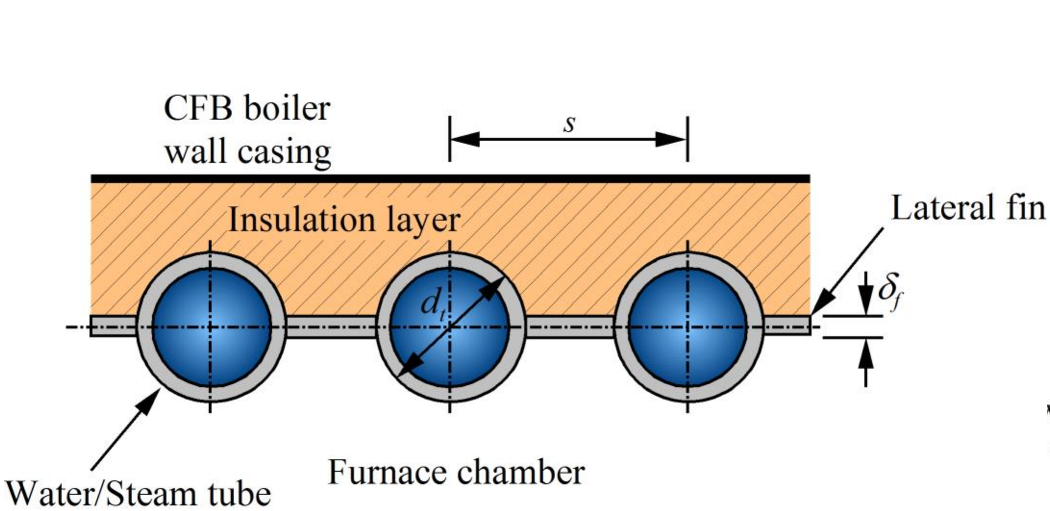

Fig. 4. Horizontal cross section of the membrane wall of CFB boiler [2].

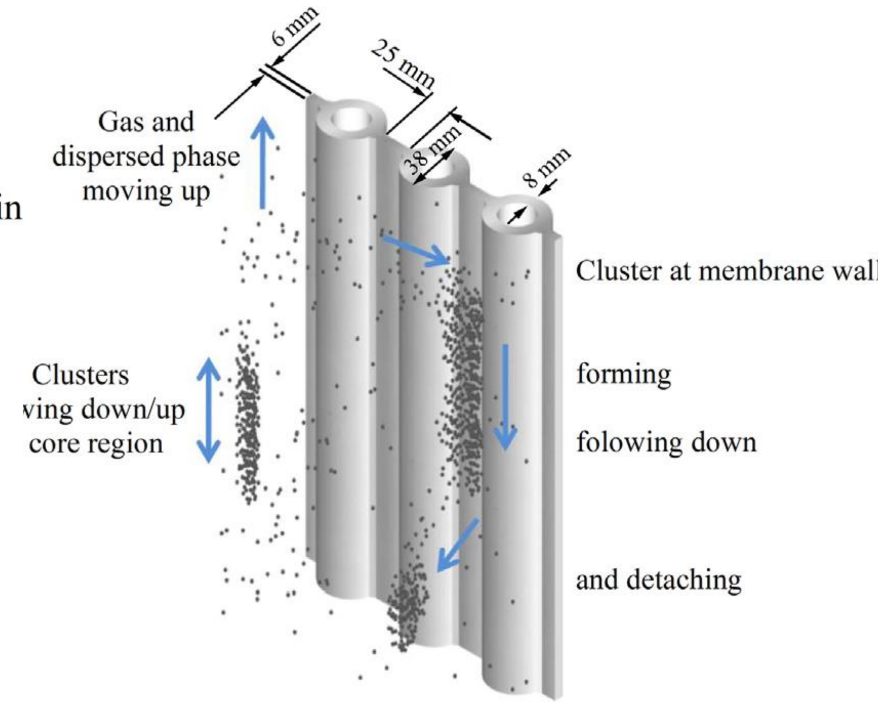

Table 1. Membrane structure for water walls.

Parameter	Symbol	Unit	Value
Tube outside diameter	d_t	mm	38
Tube pitch	s	mm	63
Lateral fin thickness	δ_f	mm	6
Ratio	ξ	-	1.24

The ratio of the contracted area to the projection area $\xi = 1.24$

$$\xi = 1 + \frac{\left[\left(\frac{\pi}{2} - 1\right) d_t - \delta_f\right]}{s}$$

[2] A. Blaszczuk, W. Nowak, Heat transfer behavior inside a furnace chamber of large-scale supercritical CFB reactor, *Int. J. Heat Mass Transfer* 87 (2015) 464–480.

MEASURING PORTS OF FURNACE DATA

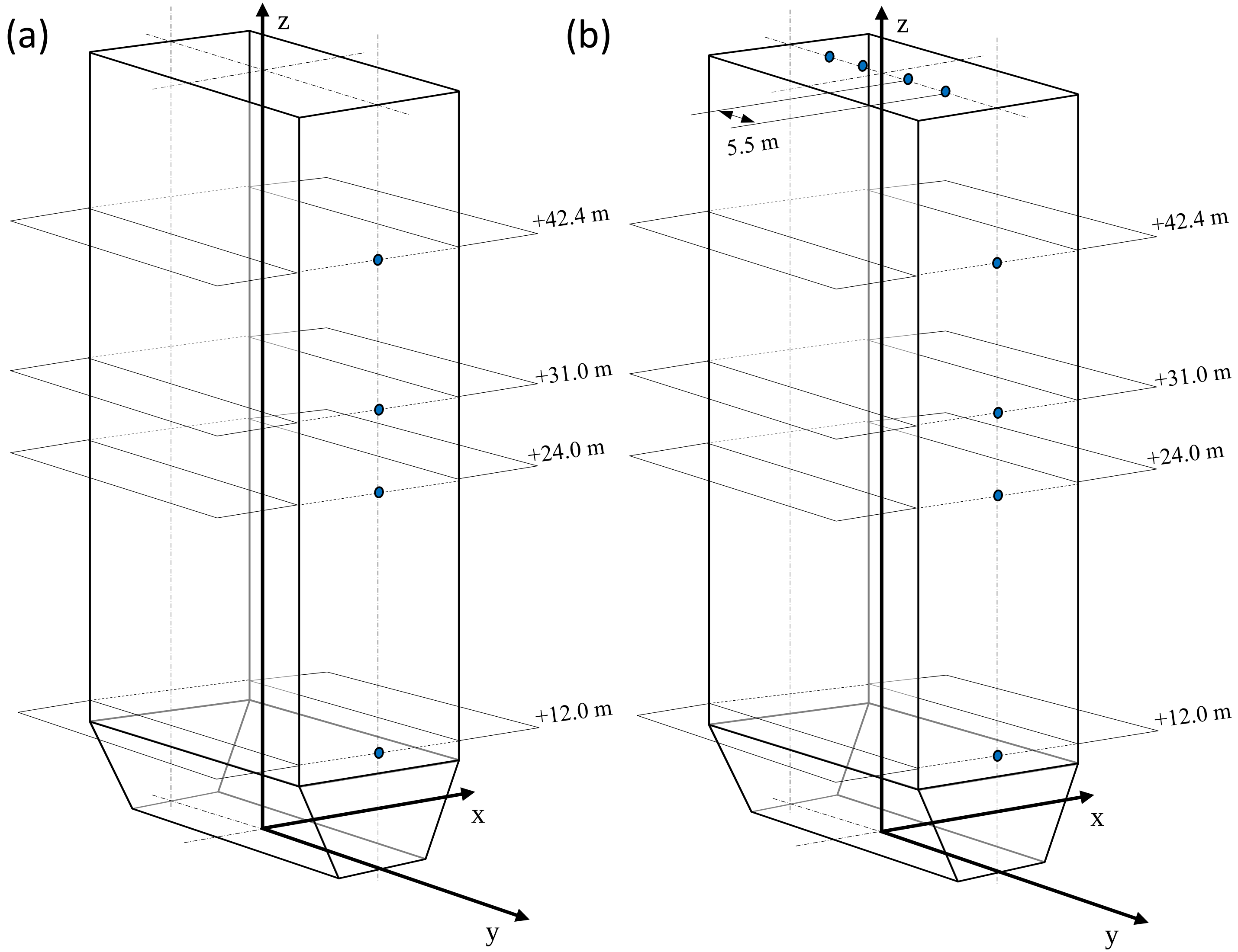

Fig. 5. Arrangement of the measuring points inside furnace chamber of 1296t/h CFB reactor: (a) pressure taps, (b) temperature ports.

 # Bed temperature – classical bare thermocouples with weights made of metal with high density and resistant to high furnace temperature.

 # Gas temperature – the shielded termocouples with insulated junction. The outside of the shield was polished. This eliminated the reflection of the membrane wall radiation.

 # Wall temperature – thermocouples at the front wall CFB furnace were imbedded in the water membrane wall with the front end flush with the fin.

[2] A. Blaszczuk, W. Nowak, Heat transfer behavior inside a furnace chamber of large-scale supercritical CFB reactor, *Int. J. Heat Mass Transfer* 87 (2015) 464–480.

EXPERIMENTAL CONDITIONS

Table 2. Experimental conditions.

Parameter	Unit	Overall range
Superficial gas velocity, U_o	m/s	2.99-5.11
Terminal velocity, U_t	m/s	1.99-2.91
Minimum fluidization velocity, U_{mf}	m/s	0.0164-0.0544
Solids circulation rate, G_s	kg/(m²s)	23.3-26.2
Sauter mean particle diameter, d_p	mm	0.219-0.411
Suspension density, ρ_b	kg/m³	1.36-6.22
Bed temperature, T_b	K	1037-1209
Wall temperature, T_w	K	700-902
Pressure drop, Δp	kPa	8.23-8.44

Table 3. Accuracies of measured parameters.

Parameters	Accuracy
Thermocouple sensor	±9°C
Temperature transmitter	±0.1°C
Pressure sensor	±2.5Pa
Stopwatch	±0.2s

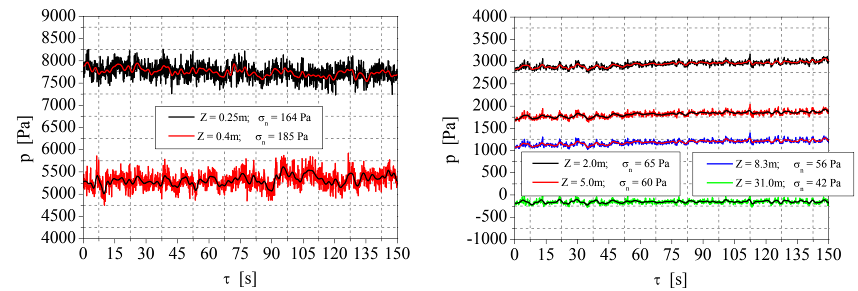

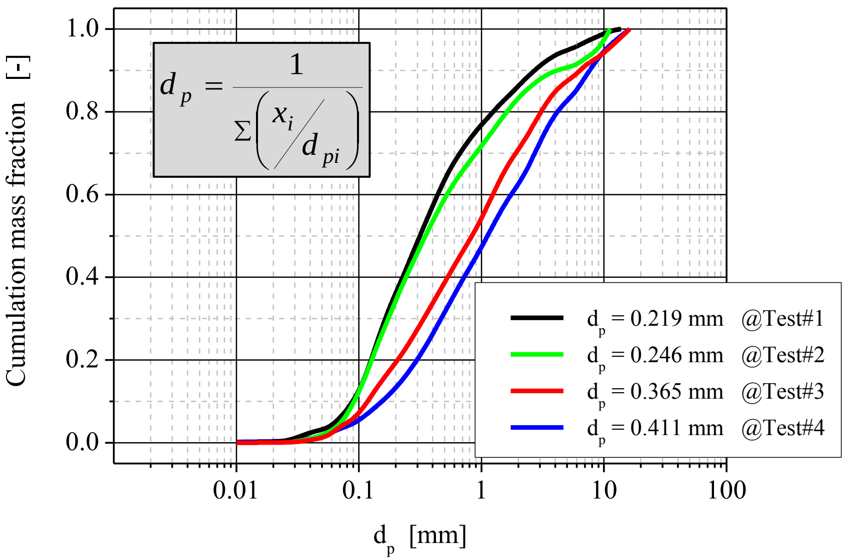

Fig. 6. Particle size distribution of bed material during performance tests.

Table 4. Fuel characteristic.

Ultimate analysis (air dried basis)	Unit	Overall range
C^{ad}, carbon	wt.%	52.32-57.09
H^{ad}, hydrogen	wt.%	4.02-4.41
O^{ad}, oxygen	wt.%	6.09-6.98
N^{ad}, nitrogen	wt.%	0.73-0.85
S^{ad}, sulphur	wt.%	0.87-1.17
Proximate analysis (as-received)		
Q^{ar}, caloric value	MJ/kg	19.91-22.91
V^{ar}, volatile matter	wt.%	24.48-29.65
A^{ar}, ash	wt.%	11.12-20.11
M^{ar}, total moisture	wt.%	13.01-19.97

RESULTS

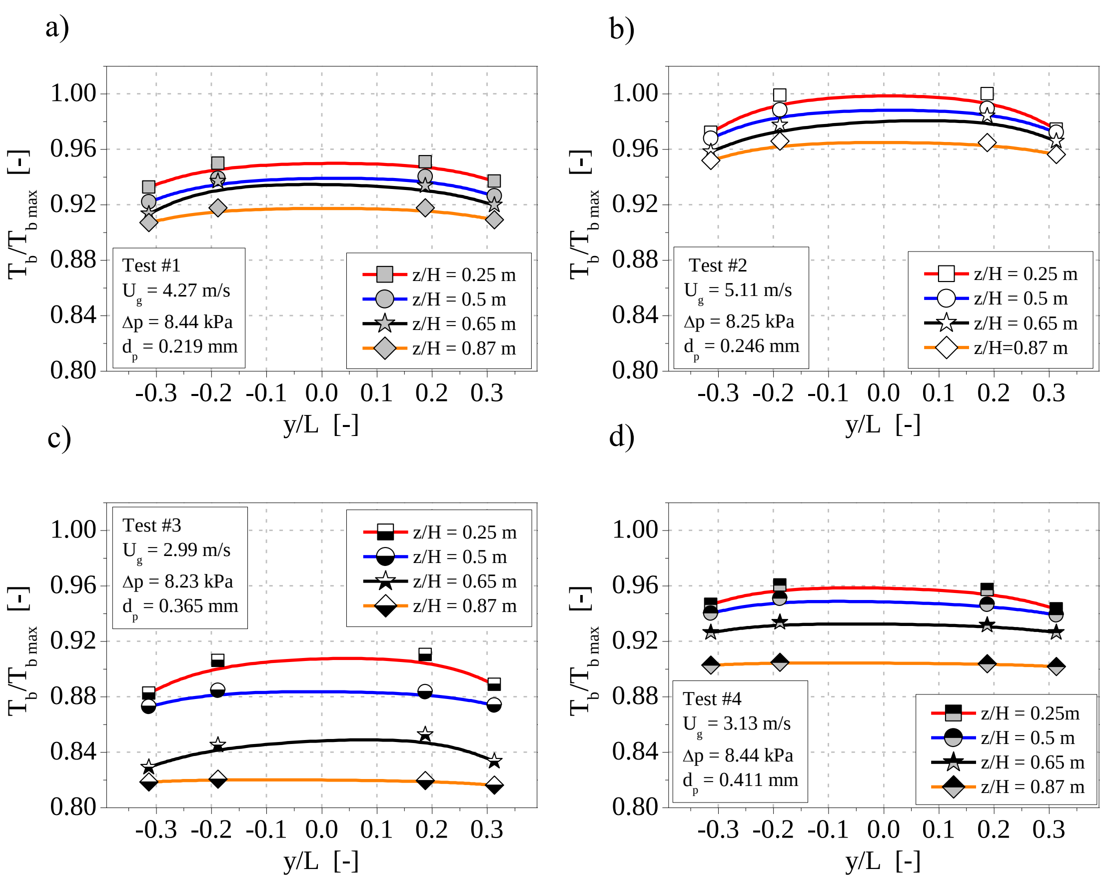

Fig. 7. Lateral temperature profiles inside furnace chamber of CFB boiler.

Table 5. Error analysis of bed temperature. (average value for each test)

Test No	Statistical parameter	
	SD	$\bar{x}$
Test #1 @ d_p=0.219mm	±8.2K	867K
Test #2 @ d_p=0.246mm	±10.4K	911K
Test #3 @ d_p=0.365mm	±7.5K	804K
Test #4 @ d_p=0.411mm	±4.4K	872K

Standard deviation *SD*

$$SD = \sqrt{\frac{\sum_{i=1}^{N}\left(x_i - \bar{x}\right)^2}{(N-1)}}$$

$$\bar{x} = \frac{1}{N}\sum_{i=1}^{N} x_i$$

Transport zone @ z/H = 0.25-0.87

RESULTS

Suspension density, ρ_b

$$\rho_b = 9.81^{-1}\left(p_i - p_{i+1}\right)\cdot\left(H_i - H_{i+1}\right)^{-1}$$

Transport zone @ z/H = 0.25-0.87

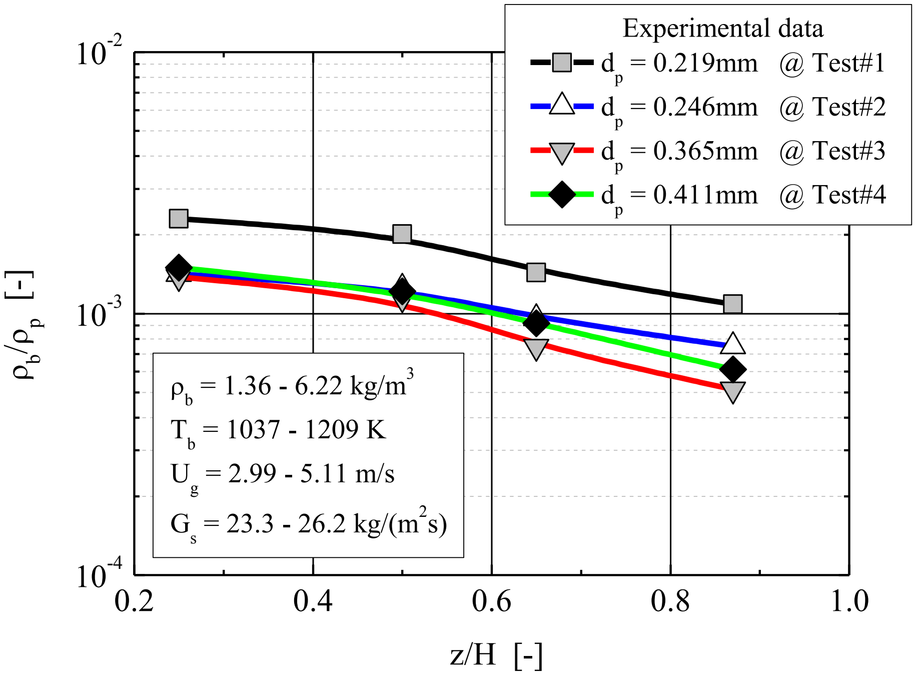

Fig. 8. Solids suspension density profiles inside furnace chamber of CFB boiler.

The root-sum-square approach (RSS)

$$\Delta x = \pm\left[\left(\left(\frac{\partial f}{\partial x_1}\right)\Delta x_1\right)^2 + \left(\left(\frac{\partial f}{\partial x_2}\right)\Delta x_2\right)^2 + \ldots + \left(\left(\frac{\partial f}{\partial x_i}\right)\Delta x_i\right)^2\right]^{1/2}$$

Table 6. Error analysis of the suspension density. (average value for each test)

Test No	Root-Sum-Square approach $\Delta\rho_b$ [kg/m^3]
Test #1 @ d_p=0.219mm	±0.41
Test #2 @ d_p=0.246mm	±0.21
Test #3 @ d_p=0.365mm	±0.22
Test #4 @ d_p=0.411mm	±0.30

RESULTS

Table 7. Relative uncertainty of the bed-to-wall heat transfer data. (average value for each test)

Test No	Relative uncertainty Δh [%]
Test #1 @ d_p=0.219mm	±18.7
Test #2 @ d_p=0.246mm	±15.8
Test #3 @ d_p=0.365mm	±11.5
Test #4 @ d_p=0.411mm	±8

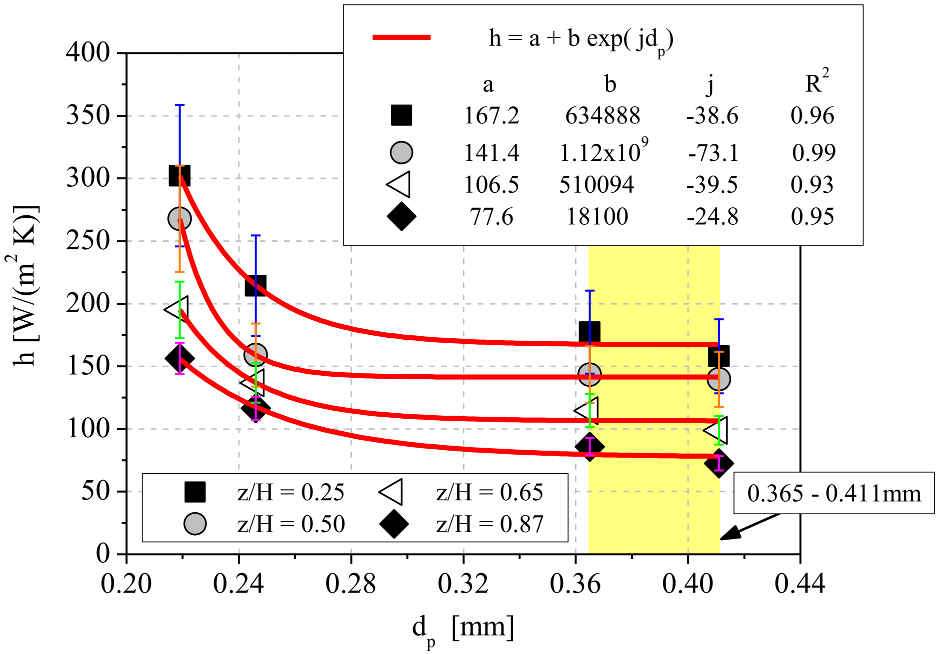

Fig. 9. Local heat transfer coefficient as a function of mean particle sizes.

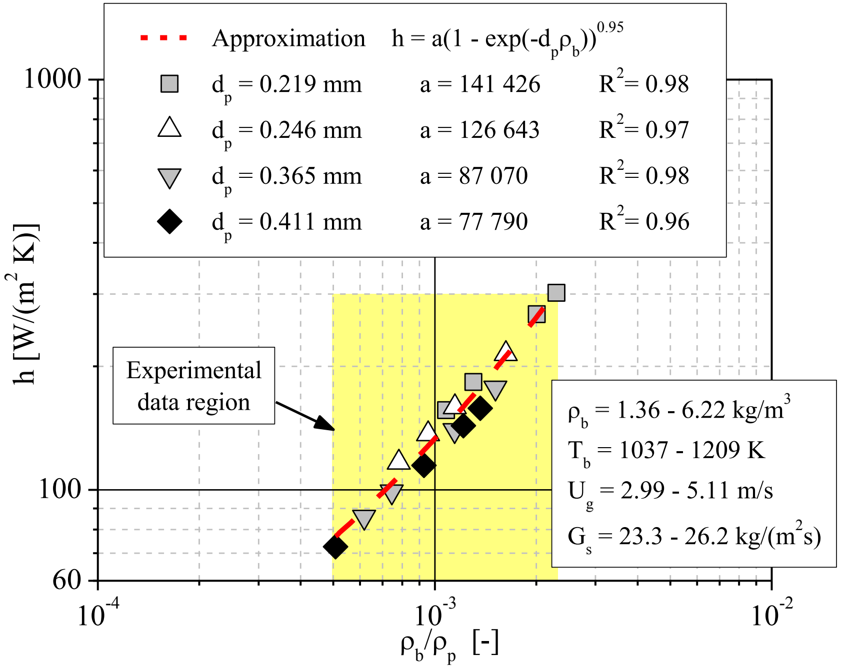

Fig. 10. Variation of bed-to-wall heat transfer coefficient versus suspension density.

RESULTS

h_{rd} / h	0.20 % – 41%
h_p / h	26% – 82%
h_{rc} / h	16% – 17%
h_g/h	0.1% – 16%

h_{rd} / h	13% – 46%
h_p / h	19% – 58%
h_{rc} / h	11% – 18%
h_g/h	8% – 22%

(a)

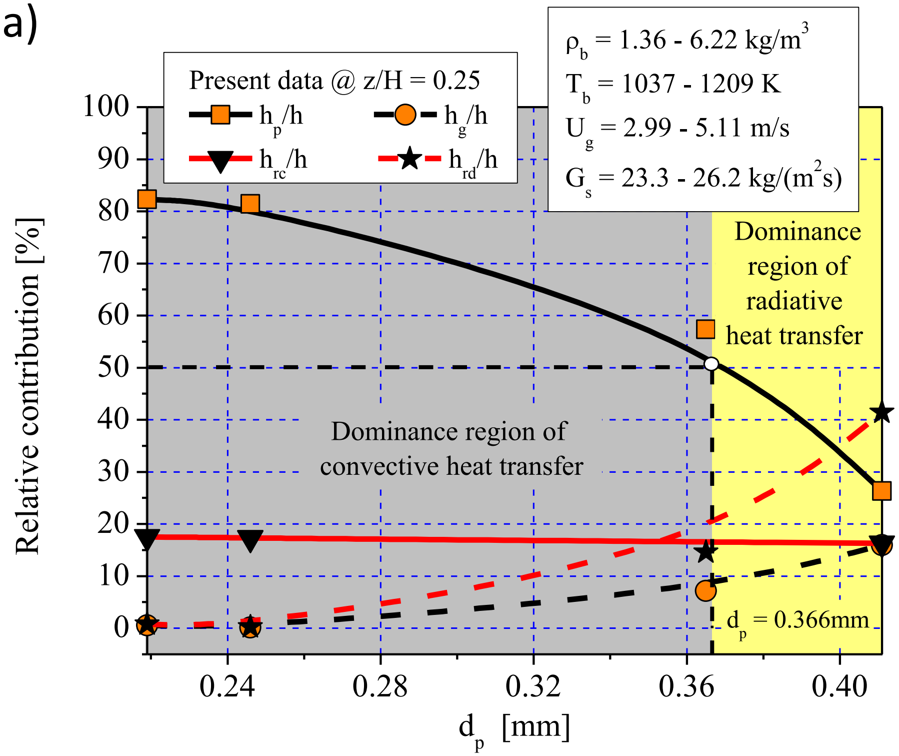

(b)

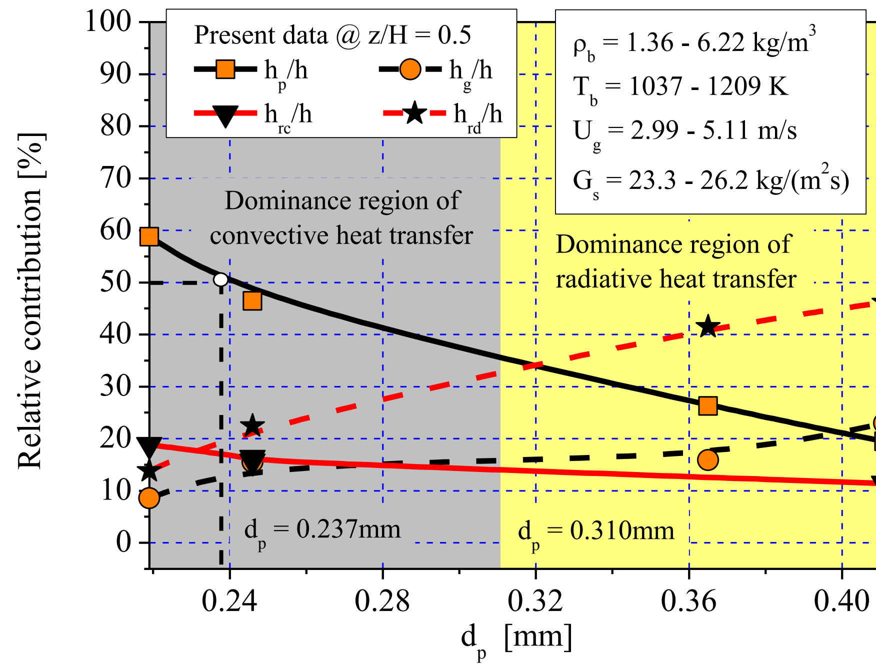

Fig. 11. Contribution of heat transfer mechanisms as a function of bed particle size inside furnace chamber: (a) at z/H=0.25, (b) at z/H=0.5.

RESULTS

(a)

h_{rd} / h	35% – 56%
h_p / h	8% – 29%
h_{rc} / h	6% – 12%
h_g/h	22% – 31%

(b)

h_{rd} / h	42% – 59%
h_p / h	5% – 20%
h_{rc} / h	4% – 10%
h_g/h	25% – 35%

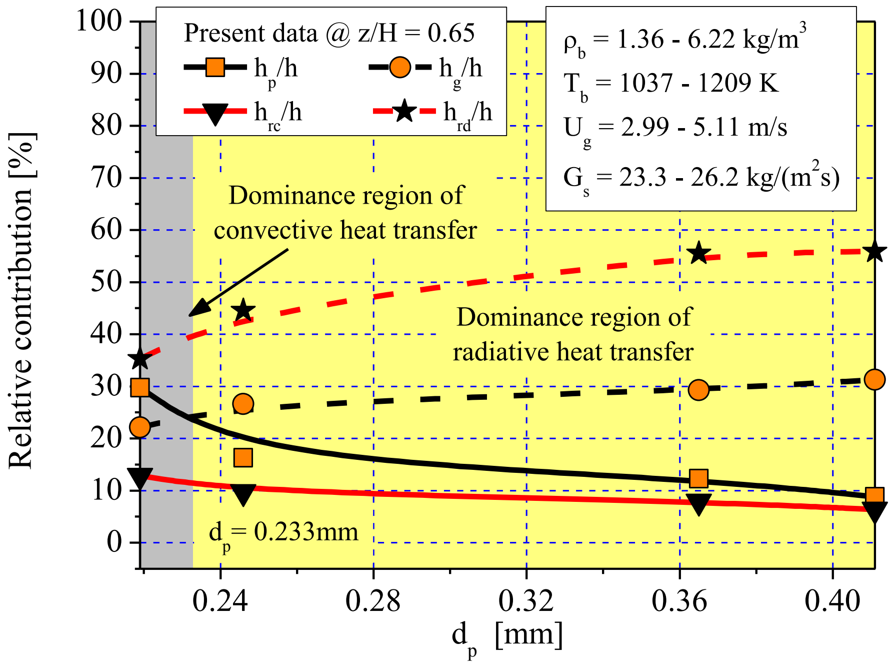

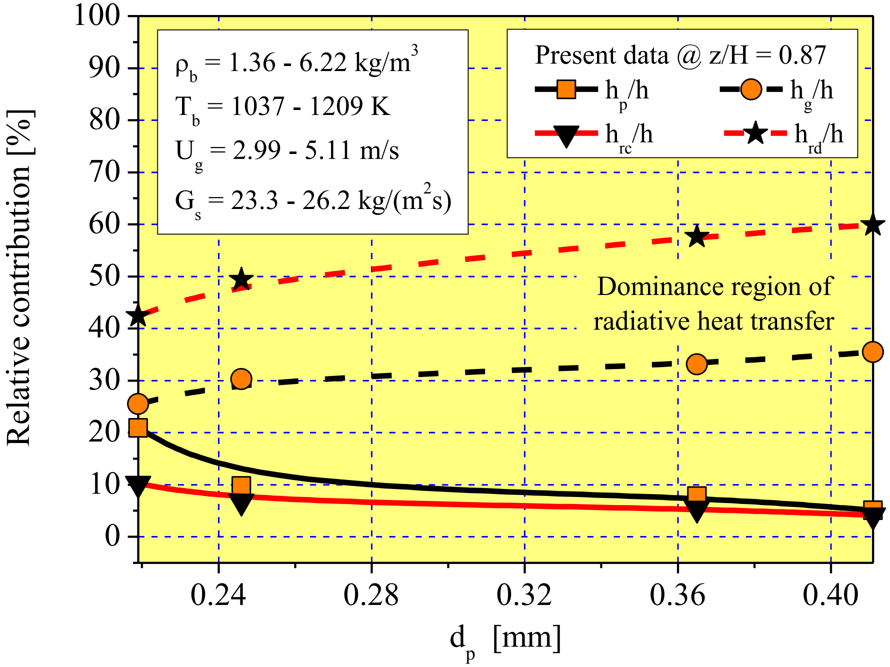

Fig. 12. Contribution of heat transfer mechanisms as a function of bed particle size inside furnace chamber: (a) at z/H=0.65, (b) at z/H=0.87.

CONCLUSIONS

The computational results exibit that:

- For the same non-dimensional distance from the grid, the smaller bed particles result in higher bed-to-wall heat transfer coefficient than larger ones. For d_p<0.241mm particles, the heat transfer coefficient increased rapidly;

- For particles tested, 0.365<d_p<0.411mm, the impact of particle diameter on local heat transfer coefficient is not important;

- The overall heat transfer coefficient is strongly dependent on particle diameter and suspension density at vertical rifled tubes,

- The bed-to-wall heat transfer coefficient increases with the decrease of bed particle size,

CONCLUSIONS

- The contribution of radiation from dispersed phase in bed-to-wall heat transfer coefficient increased with the increase in bed particle size, especially for coarse bed particles with diameter d_p>0.365mm

- With increase in bed particle diameter, cluster radiation component in the heat transfer mechanism gradually decreases along the furnace height,

- For all particle tested, 0.240<d_p<0.411mm, the bed particle diameter had an essential impact on gas convection heat transfer and cannot be ignored,

Czestochowa University of Technology,
Institute of Advanced Energy Technologies
ul. Dabrowskiego 73, 42-200 Czestochowa, POLAND

Thank you for your attention

The authors would like to gratefully acknowledge the staff of Tauron Generation S.A. Lagisza Power Plant for technical support with supplying operating data and construction data. This work was financially supported by Scientific Research Grant *No BS-PB-406/301/11* funded by Polish Ministry of Science and Higher Education.